

Role of Sodium Channel Deglycosylation in the Genesis of Cardiac Arrhythmias in Heart Failure*

Received for publication, March 21, 2001, and in revised form, May 3, 2001
Published, JBC Papers in Press, May 21, 2001, DOI 10.1074/jbc.M102548200

Carmen A. Ufret-Vincenty^{‡§}, Deborah J. Baro^{‡¶}, W. Jonathan Lederer^{**}, Howard A. Rockman^{‡‡}, Luis E. Quiñones[‡], and L. Fernando Santana^{‡§§}

From the [‡]Institute of Neurobiology, University of Puerto Rico, San Juan, Puerto Rico 00901, the [¶]Department of Biochemistry, Medical Sciences Campus, University of Puerto Rico, San Juan, Puerto Rico 00936, the ^{**}Medical Biotechnology Center and Department of Physiology, University of Maryland School of Medicine, Baltimore, Maryland 21201, and the ^{‡‡}Department of Medicine and Cell Biology, Duke University Medical Center, Durham, North Carolina 27710

We investigated the cellular and molecular mechanisms underlying arrhythmias in heart failure. A genetically engineered mouse lacking the expression of the muscle LIM protein (MLP^{-/-}) was used in this study as a model of heart failure. We used electrocardiography and patch clamp techniques to examine the electrophysiological properties of MLP^{-/-} hearts. We found that MLP^{-/-} myocytes had smaller Na⁺ currents with altered voltage dependencies of activation and inactivation and slower rates of inactivation than control myocytes. These changes in Na⁺ currents contributed to longer action potentials and to a higher probability of early afterdepolarizations in MLP^{-/-} than in control myocytes. Western blot analysis suggested that the smaller Na⁺ current in MLP^{-/-} myocytes resulted from a reduction in Na⁺ channel protein. Interestingly, the blots also revealed that the α -subunit of the Na⁺ channel from the MLP^{-/-} heart had a lower average molecular weight than in the control heart. Treating control myocytes with the sialidase neuraminidase mimicked the changes in voltage dependence and rate of inactivation of Na⁺ currents observed in MLP^{-/-} myocytes. Neuraminidase had no effect on MLP^{-/-} cells thus suggesting that Na⁺ channels in these cells were sialic acid-deficient. We conclude that deficient glycosylation of Na⁺ channel contributes to Na⁺ current-dependent arrhythmogenesis in heart failure.

Cardiac arrhythmias are a leading cause of death among patients with HF¹ (1). However, the cellular and molecular changes in cardiac myocytes with contractile dysfunction

leading to arrhythmias are not clear (2). Recent work suggests that action potential (AP) prolongation is a major contributing factor to the increased probability of cardiac arrhythmias observed in HF. The cellular and molecular processes that underlie AP prolongation have been attributed to the following: 1) altered K⁺ channel currents (3–11), 2) changes in Na⁺ channel currents (12–15), and 3) altered Ca²⁺ signaling (16–18). These alterations are often brought about by changes in the amount or identity of specific ion channels or Ca²⁺-signaling proteins (11, 19, 20). In addition, it has been suggested that alterations in post-translational modification of proteins, specifically reduced glycosylation, could also contribute to HF and related conditions (21). The molecular mechanisms underlying these perturbations in protein expression and processing during HF have remained unclear.

The purpose of this study was to investigate the molecular causes of AP prolongation and arrhythmias in HF. The muscle LIM protein “knockout” mouse (MLP^{-/-}) (2, 22–24) was used as a model of HF because it has been examined extensively by multiple groups and found to have reproducible HF. Furthermore, the MLP^{-/-} mouse reproduces many of the morphological and clinical features of HF in humans (22, 25). We found that during HF, Na⁺ currents (I_{Na}) are modified in ways that cause action potential prolongation and arrhythmogenesis. Our data suggest that these changes in I_{Na} are caused by deficient glycosylation of the Na⁺ channel protein during HF. We conclude that incomplete glycosylation during post-translational processing contributes to Na⁺ channel-dependent arrhythmogenesis in HF.

EXPERIMENTAL PROCEDURES

Isolation of Cardiac Myocytes—Adult animals (25 g) were euthanized with an intraperitoneal injection of pentobarbital (100 mg/kg) in strict accordance to the guidelines established by the Institutional Animal Care and Use Committee, which follows all applicable state and federal laws. Single mouse ventricular myocytes were isolated as described previously (26) and stored at room temperature (22–25 °C) in Dulbecco's modified Eagle's medium (Sigma) until used.

ECG Measurements—ECGs were recorded from diazepam-sedated (15 mg/kg) WT and MLP^{-/-} mice using methods described previously (27). A differential amplifier (Warner Instruments, Hamden, CT) was used to record any one of the six bipolar limb leads in standard fashion. Data were digitized at 2 kHz with a Digidata 1320 A/D converter (Axon Instruments, Foster City, CA) and stored in a computer running Axotape software (Axon Instruments, Foster City, CA). Analysis was performed in signal-averaged beats. To do this the first 20 beats recorded were aligned with respect to their R peak and then averaged. QT intervals were calculated using the lead with the most prominent T wave (usually lead 1). Correction of the QT interval for heart rate (QT_c) was performed using Equation 1 (28),

* This work was supported by NINDS Grants 1 U54 NS39405-02 (to L. F. S.), RO1 NS38770 (to D. J. B.), RO1 HL67927 (to L. F. S.), NSF-EPSCoR (to L. F. S. and D. J. B.), and RCMI-UPR G12RR-03051 (to L. F. S. and D. J. B.) from the National Institutes of Health. The costs of publication of this article were defrayed in part by the payment of page charges. This article must therefore be hereby marked “advertisement” in accordance with 18 U.S.C. Section 1734 solely to indicate this fact.

§ Current address: Dept. of Physiology and Biophysics, University of Washington, Box 357290, Seattle, WA 98195-7290.

¶ Current address: Dept. of Biology, Georgia State University, 24 Peach Tree Ave., Atlanta, GA 30303.

§§ To whom correspondence should be addressed. Tel.: 787-724-2059; Fax: 787-721-5474; E-mail: lsantana@neurobio.upr.clu.edu.

¹ The abbreviations used are: HF, heart failure; AP, action potential; APD₉₀, action potential duration at 90% repolarization; MLP, muscle LIM protein; WT, wild type; MLP^{-/-}, MLP knockout; G, conductance; G_{max}, maximal conductance; ECG, electrocardiogram; EAD, early afterdepolarization; QT_c, heart rate-corrected QT interval; LQTS, long QT syndrome.

$$QT_c = \frac{QT}{\sqrt{RR/100}} \quad (\text{Eq. 1})$$

where QT_c is the corrected QT interval and RR is the interval between R peaks.

Electrophysiology—During experiments, cells were continuously superfused with a solution (solution A) containing the following constituents (in mM): 135 NaCl, 5 KCl, 2 CaCl₂, 1 MgCl₂, 10 HEPES, 10 glucose, pH 7.4. Myocytes were patched in this solution, and after a gigaohm seal was formed, a small amount of negative pressure was applied through the patch pipette to break the membrane and achieve the whole-cell configuration of the patch clamp technique. I_{Na} were measured while cells were bathed with an external solution containing the following (in mM): 10 NaCl, 130 CsCl, 0.5 CaCl₂, 2.5 MgCl₂, 0.1 CdCl₂, 0.1 NiCl₂, 10 HEPES, 10 glucose, pH 7.4. The patch pipette was filled with a solution containing the following (in mM): 130 CsCl, 10 NaCl, 10 HEPES, 4 ATP-Mg, 5 EGTA, pH 7.3. APs were recorded while cells were continuously superfused with solution A. For these experiments patch pipettes were filled with a solution with the following constituents (in mM): 110 K-Asp; 20 KCl, 10 NaCl, 4 ATP-Mg, 10 HEPES, pH 7.3. I_{Na} and APs were recorded at room temperature (22–25 °C) using an Axopatch 200B amplifier (Axon Instruments) and pCLAMP 8 software (Axon Instruments). APs were triggered by a 2-ms injection of a depolarizing 2-nA current at a frequency of 1 Hz.

Analysis of APs and I_{Na} was performed using Clampfit 8 software (Axon Instruments, Foster City, CA). Normalization of ventricular Na⁺ currents was performed by dividing them by the capacitance (in pF) of the cell from which they were recorded. Cell capacitance was measured using the membrane test module of Clampex 8.0. I_{Na} conductance was determined according to Equation 2,

$$G = \frac{I}{(V_{test} - V_{rev})} \quad (\text{Eq. 2})$$

where G is the conductance of sodium; I is the measured current; V_{test} is the test potential at which the current was measured, and V_{rev} is the calculated Nernst equilibrium potential of Na⁺ (0 mV).

Analysis was performed on I_{Na} that met three criteria. First, the amplitude of I_{Na} could not exceed 3 nA. Second, there were no abrupt increments in I_{Na} during the increasing phase of the current-voltage relationship. Third, the series resistance was not larger than 3 megohms.

Protein Isolation and Western Blots—WT and MLP^{-/-} hearts were isolated and stored at -70 °C. Whole hearts were homogenized at 4 °C with a Tissuizer (Tekmar, Cincinnati, OH) in TE (50 mM Tris, pH 7.5; 1 mM EDTA) containing the following protease inhibitors: 10 μg/ml leupeptin, 10 μg/ml pepstatin, 2 μg/ml aprotinin, 1 mM benzamide, 10 μg/ml calpain inhibitor I, 20 μg/ml calpain inhibitor II, 1 mM Pefabloc-SC plus protector, 50 μg/ml antipain, 2 mM phenanthroline, 5 mM iodoacetamide. The homogenate was stored on ice, and SDS (0.5%, w/v) and Triton X-100 (2%, v/v) were added. Proteins were solubilized by shaking 1–2 h at 4 °C. Insolubilized material was pelleted by centrifugation at 13,000 × g for 20 min, and 100-μl aliquots of the supernatant were stored at -70 °C. Protein concentrations were determined with the Lowry method. Protein samples were mixed with 3× loading buffer (58% glycerol, 0.36 M Tris, pH 6.8, 6% SDS, 6% β-mercaptoethanol, 0.006% bromophenol blue) and heated to 42 °C for 20–30 min. Protein samples were loaded onto 5–6% discontinuous gels and resolved with SDS-polyacrylamide gel electrophoresis. Equal amounts of MLP^{-/-} and WT proteins were loaded in multiple lanes. Two control and two MLP^{-/-} mice were used in these experiments. Proteins were transferred to polyvinylidene difluoride-plus membranes (Osmonics, Westborough, MA) at 45 mA for 4 h using a semidry electroblotter (Owl Scientific). Membranes were used for Western blot analysis as described previously (29). Polyclonal antibodies against the α-subunit of the Na⁺ channel were obtained from Upstate Biotechnology Inc. (Lake Placid, NY) and Alomone Laboratories (Jerusalem, Israel) and used at the recommended concentration. Both antibodies recognized the same Na⁺ channel smear whose lower boundary was the predicted molecular weight of the α-subunit of the Na⁺ channel protein (~220 kDa). The Na⁺ channel smears produced by both antibodies could be blocked by pre-absorption of the antibody with the peptide antigen. In addition, each antibody produced a unique set of lower molecular weight bands that could not be blocked by pre-absorption with the antigen. The intensity of these nonspecific bands did not vary between control and mutant mice and served as convenient markers for normalization of the Na⁺ channel signal. Optical densities for antibody signals were determined with Gel Expert software (Nucleotech, Hayward, CA).

Statistics—Data are presented as means ± S.E. Two sample comparisons were performed using Student's *t* test. When multigroup comparisons were necessary they were made using a one-way analysis of variance followed by a Tukey's test. In all tests a *p* value smaller than 0.05 was considered an indicator of a significant difference between groups.

RESULTS

Action Potential Prolongation and Early Afterdepolarizations in MLP^{-/-} Cells—We examined the electrical activity of ventricular myocytes with HF and contractile dysfunction using whole animal electrocardiograph (ECG) measurements and single cell APs. The electrical properties of the MLP^{-/-} mouse heart are compared with those of WT mouse hearts in Fig. 1. ECGs taken from adult mice showed signs of abnormal electrical activity in the MLP^{-/-} animals (Fig. 1A). Specifically, MLP^{-/-} mice had QT intervals (87.56 ± 6.56 ms, $n = 5$) that were significantly longer than those observed in WT mice (46.57 ± 4.76 ms, $n = 7$; $p = 0.01$). This difference in QT interval between WT and MLP^{-/-} mice was still significant after correcting it for the heart rate (QT_c interval) of each animal (40.24 ± 4.78 ms in WT versus 77.50 ± 6.56 in MLP^{-/-}, $p = 0.02$).

Because long QT intervals are caused largely by prolonged APs, our data suggest that MLP^{-/-} myocytes have longer APs than WT myocytes. To test this hypothesis, APs were recorded in WT and MLP^{-/-} myocytes using the current clamp method. In these experiments single WT and MLP^{-/-} ventricular myocytes were stimulated through the patch pipette at 1 Hz. Representative APs from MLP^{-/-} and WT myocytes are shown superimposed in Fig. 1B. In MLP^{-/-} cells the prolonged APs were largely associated with a slowing of rapid repolarization (phase 1) and an increase in the plateau (phase 2). The *inset*, showing bar graphs for the AP duration at 90% repolarization (APD_{90}), reveals that the AP was significantly longer in MLP^{-/-} (210.75 ± 52.88 ms, $n = 15$) than in WT myocytes (41.56 ± 10.75 ms, $n = 25$; $p = 0.01$).

To investigate the arrhythmogenic potential of the prolonged APs in MLP^{-/-} animals, myocytes were stimulated at 1 Hz for periods of 1 min. Clusters of 5 APs from WT and MLP^{-/-} records are shown in Fig. 1C. Arrhythmogenic voltage fluctuations called early afterdepolarization (EADs, Fig. 1C) were frequently observed in the MLP^{-/-} cells. Indeed, Fig. 1D illustrates that the probability of observing early afterdepolarizations in MLP^{-/-} cells ($25 \pm 3\%$; $n = 15$) was significantly higher than in WT cells ($2 \pm 1\%$, $n = 25$, $p < 0.001$).

Altered Membrane Current in MLP^{-/-} Myocytes—The longer QT intervals we observed in MLP^{-/-} mice resemble the long QT syndrome (LQTS) in humans. In some LQTS, mutations in Na⁺ channel proteins lead to alterations in I_{Na} that have been associated with increases in AP duration and cardiac arrhythmias (13, 16). Although there is no mutation in the Na⁺ channel gene in MLP^{-/-} mice, the changes in AP shape that we observed experimentally in Fig. 1 suggested to us that a change in I_{Na} could account for the changes in the AP and arrhythmias seen in the MLP^{-/-} heart.

If changes in I_{Na} contribute to the development of the LQTS in the MLP^{-/-} model of HF, then specific changes in I_{Na} should be clear and reproducible. Fig. 2 shows the results of a series of experiments that compared the biophysical properties of I_{Na} in WT and MLP^{-/-} myocytes. The current-voltage (IV) relationship for I_{Na} of ventricular myocytes isolated from WT and MLP^{-/-} hearts is shown in Fig. 2A. The data indicate a lower I_{Na} density in MLP^{-/-} than in WT myocytes. The peak I_{Na} was reduced by $35 \pm 5\%$ ($n = 6$, $p < 0.001$) in the MLP^{-/-} myocytes with a shift in the IV relationship toward more positive potentials. This shift is more clearly revealed in Fig. 2B, where the normalized conductance (G/G_{max}) is plotted as a function of voltage. The half-maximal conductance is significantly shifted

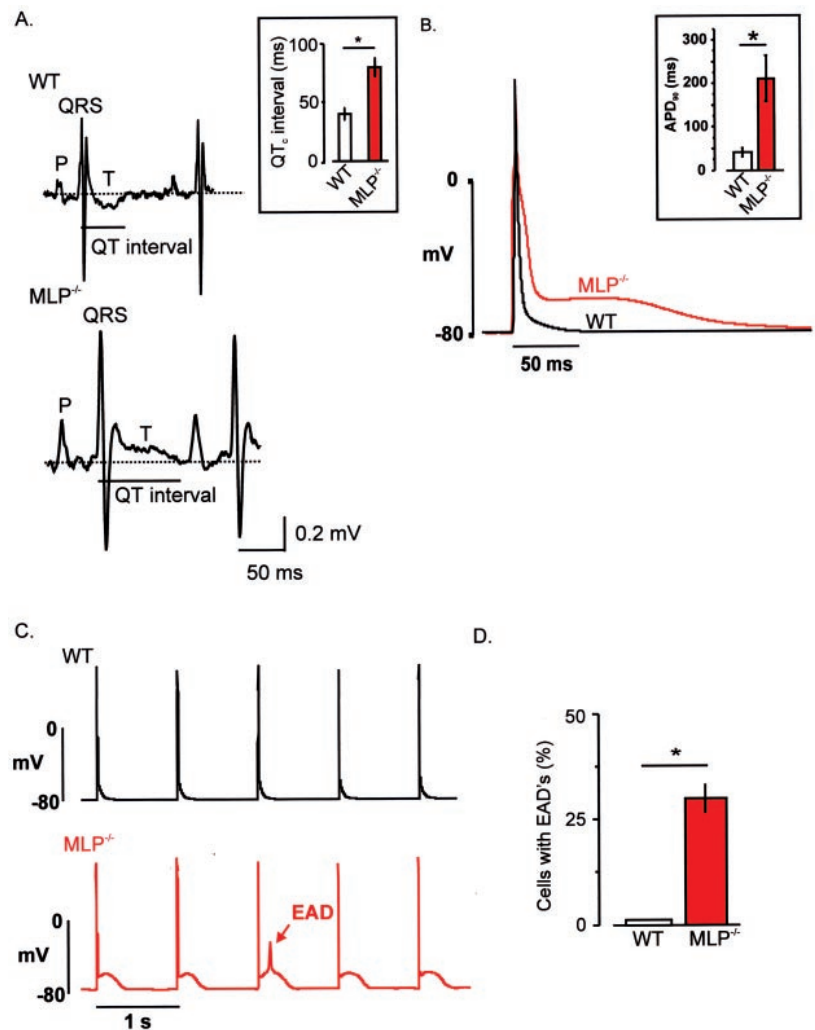


FIG. 1. Lengthening of the action potential of cardiac myocytes and increase in the probability of arrhythmias during heart failure. A, MLP^{-/-} mice have longer QT intervals than WT mice. Shown in this panel are two ECGs recorded from a representative WT (top) and MLP^{-/-} (bottom) mouse. The inset shows a bar plot of the mean \pm S.E. of the QT_c interval in WT and MLP^{-/-} mice. B, this panel shows two representative action potentials (AP) recorded from WT (black line) and MLP^{-/-} (red line) myocytes. The inset in this panel shows the average action potential duration at 90% (APD₉₀) repolarization in WT ($n = 8$) and MLP^{-/-} ($n = 7$) myocytes. C, representative AP trains in WT (top trace) and MLP^{-/-} (bottom trace) myocytes. The arrow points to an EAD. D, bar plot of the percentage of cells showing EADs during periods of sustained AP stimulation (30–60 s) at a frequency of 1 Hz.

by 12 mV from -49.64 ± 0.13 mV ($n = 6$) to -37.76 ± 0.28 mV ($n = 6$; $p < 0.001$). Additionally, the voltage dependence of the steady-state inactivation of I_{Na} in MLP^{-/-} myocytes is shifted 7 mV in the negative direction from -80.66 ± 0.49 mV to -86.20 ± 0.36 mV ($p = 0.01$) as is shown in Fig. 2C. Fig. 2C also shows that there was a clear slowing of inactivation of I_{Na} in the MLP^{-/-} myocytes. Indeed, the inactivation time constant ($\tau_{\text{inactivation}}$) of I_{Na} in MLP^{-/-} myocytes was about 50% greater than in WT myocytes.

These alterations in I_{Na} in the MLP^{-/-} mouse ventricular myocyte raise two important questions. First, how are the changes in I_{Na} produced? Second, are the changes in I_{Na} sufficient to produce the observed changes in AP shape?

Deglycosylation of Na^+ Channels in HF—The Na^+ channel gene is not mutated in MLP^{-/-} mice. Thus, if the changes in I_{Na} in MLP^{-/-} are due to changes in gene expression and/or protein processing, the Na^+ channel could be modified in many different ways. Indeed, down-regulation of Na^+ channel expression levels could account for the 35% reduction in the density of I_{Na} (see above) but not for the shifts in its voltage dependence. On the other hand, improper processing of the channel protein could account for one or both of these effects.

To determine if Na^+ channel expression levels were altered in MLP^{-/-} mice, we performed Western blot analysis of the α -subunit of the cardiac Na^+ channel. Fig. 3 illustrates that there is a statistically significant $34.27 \pm 0.07\%$ ($n = 12$, $p < 0.001$) reduction in the intensity of the Na^+ channel band in MLP^{-/-} hearts relative to WT. These data suggest that there is significant reduction in Na^+ channel protein during HF and

that the smaller I_{Na} density observed in MLP^{-/-} cells (Fig. 2) results from a lower number of functional Na^+ channels expressed in these cells.

Close examination of the Western blots showed that the α -subunit of Na^+ channels is heavily glycosylated, as the signal appears as a smear above the predicted molecular weight of this glycoprotein (≈ 220 kDa), rather than a single sharp band (Fig. 3). The blots also revealed that the width of the Na^+ channel band was significantly narrower in MLP^{-/-} than in WT hearts. Indeed, the width at 50% of the amplitude of the Na^+ channel band was significantly smaller ($21 \pm 6\%$, $p < 0.05$, $n = 7$) in MLP^{-/-} than in WT hearts (Fig. 3). The reduction in width reflects a loss in the higher molecular weight species. Thus, these data suggest that in the MLP^{-/-} heart, heavily glycosylated, high molecular weight Na^+ channels are less abundant than in the WT heart, resulting in a reduction in the average molecular weight of the Na^+ channel protein during HF.

Interestingly, the peak and leading edge of the Na^+ channel from the MLP^{-/-} heart tended to migrate further in the gel ($12 \pm 5\%$, $n = 7$) than the Na^+ channel of the WT heart. However, this shift in the peak and leading edge of the Na^+ channel band was not statistically significant, a finding that, based on the work of others (30), is not unexpected. The position of the peak reflects the molecular weight of the most abundant species. Thus, these data suggest that the most abundant species of Na^+ channel proteins have similar molecular weights in WT and MLP^{-/-} myocytes. However, the position of the peak provides little information about the average

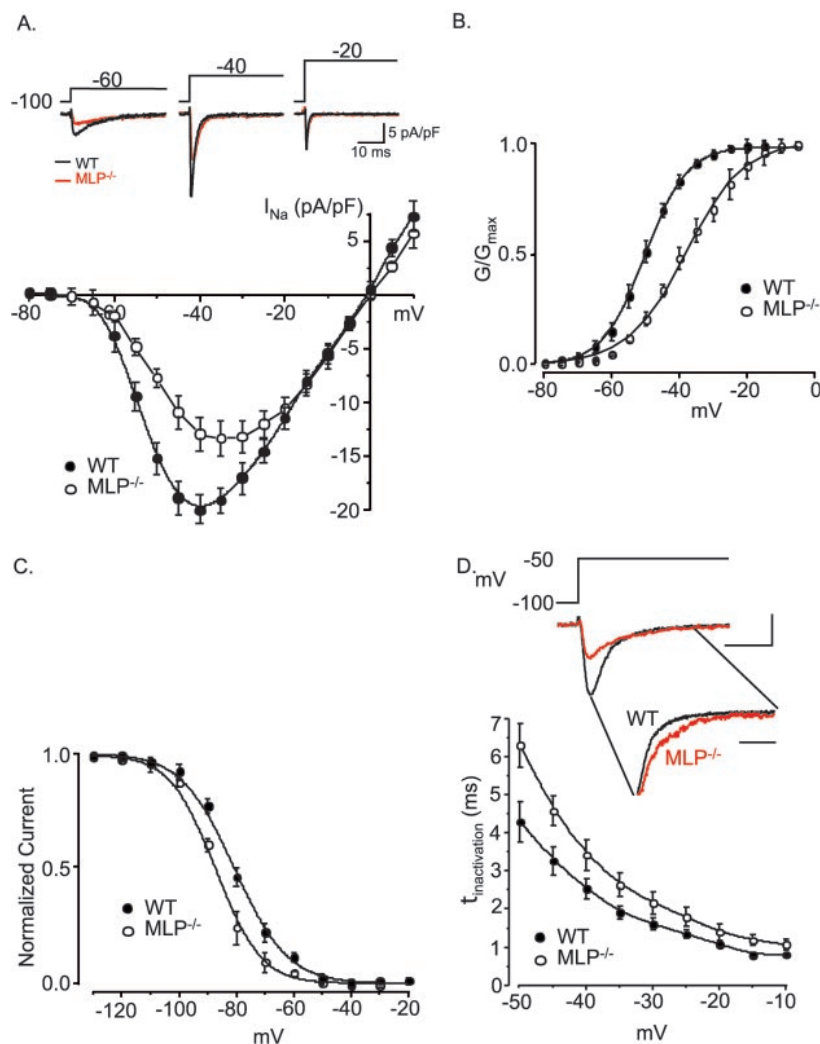


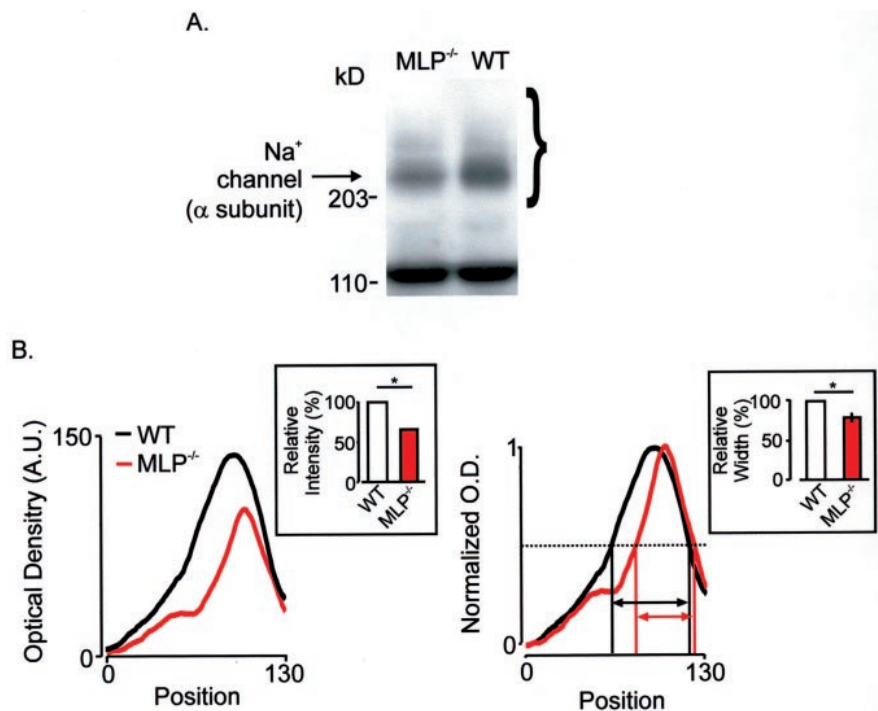
FIG. 2. Modification of I_{Na} during HF. A, IV relationship of I_{Na} in WT and $\text{MLP}^{-/-}$ myocytes. At the top of this panel a family of representative I_{Na} traces from WT (black lines) and $\text{MLP}^{-/-}$ (red line) cells are shown. These I_{Na} were evoked by 50-ms voltage steps from the holding potential of -100 to -60 (left), -40 (middle), and -20 mV (right). The graph summarizes the IV relationships of I_{Na} from six WT and $\text{MLP}^{-/-}$ cells. B, voltage dependence of the normalized conductance (G/G_{max}) of I_{Na} in WT and $\text{MLP}^{-/-}$ myocytes. The curves in this graph are the best-fit line determined by a least squares method using a Boltzmann equation, $y = (A_1 - A_2)/(1 + e^{(x-V_{1/2})/dV})$, where A_1 , A_2 , $V_{1/2}$, and dV are the initial value, final value, the center, and the slope factor. For WT, $A_1 = 0.98$, $A_2 = 0.01$, $V_{1/2} = -50.25$ mV, and $dV = 5.98$; and for $\text{MLP}^{-/-}$, $A_1 = 0.97$, $A_2 = 0.02$, $V_{1/2} = -38.15$ mV, and $dV = 8.64$. C, voltage dependence of the steady-state inactivation of I_{Na} in WT and $\text{MLP}^{-/-}$ myocytes. The voltage protocol used to generate these data involved a 200-ms pre-pulse to voltages ranging from -130 to -20 mV after which a 30-ms pulse to -40 mV was applied. The curves in this graph were obtained as in B. For WT, $A_1 = 1.03$, $A_2 = 0.03$, $V_{1/2} = -80.45$ mV, and $dV = 8.42$; and for $\text{MLP}^{-/-}$, $A_1 = 0.99$, $A_2 = 0.03$, $V_{1/2} = -87.10$ mV, and $dV = 6.89$. D, voltage dependence of the rate of inactivation of I_{Na} in WT and $\text{MLP}^{-/-}$ myocytes. The top portion of this panel shows two representative I_{Na} records obtained in WT (black line) and $\text{MLP}^{-/-}$ (red line) during a step depolarization to -50 mV from the holding potential of -100 mV. The lines radiating from these I_{Na} traces demarcate the region in these traces that are normalized and zoomed and that are shown below. Note that WT I_{Na} inactivates much faster than the I_{Na} recorded in $\text{MLP}^{-/-}$ cells. The voltage dependence of the $\tau_{\text{inactivation}}$ of I_{Na} in WT (\bullet , $n = 6$) and $\text{MLP}^{-/-}$ (\circ , $n = 6$) cells is shown at the bottom of this panel.

molecular weight of the Na^+ channel protein, which depends directly on the average glycosylation of these channels in these cells.

Our Western blot analysis suggests that a reduction in the glycosylation of Na^+ channel proteins during post-translational processing could underlie the changes in I_{Na} observed in $\text{MLP}^{-/-}$ myocytes. Indeed, the extent of Na^+ channel glycosylation has been shown to affect broadly the function of this channel (30, 31). To investigate if a reduction in glycosylation of Na^+ channel proteins during post-translational processing was responsible for the changes in I_{Na} observed in $\text{MLP}^{-/-}$ myocytes, both control and $\text{MLP}^{-/-}$ cells were exposed to neuraminidase, an enzyme known to reduce extracellular glycosylation when applied to the solution bathing cells (30). Myocytes were treated for 3 h at room temperature (23–25 °C) with 0.3 units/ml of neuraminidase. We found that neuraminidase produced a shift of about 10 mV in the voltage at which the peak

I_{Na} occurred in WT cells (Fig. 4A). This shift in the current-voltage relationship of I_{Na} in neuraminidase-treated WT cells is similar to the one observed in $\text{MLP}^{-/-}$ cells. Note, however, that neuraminidase did not produce any shift in the current-voltage relationship of I_{Na} in $\text{MLP}^{-/-}$ myocytes. As expected from these results, neuraminidase shifted the voltage dependence of the relative conductance of I_{Na} in WT cells but not in $\text{MLP}^{-/-}$ cells (Fig. 4B). This positive shift in the conductance voltage relationship of I_{Na} in neuraminidase-treated WT cells is identical to that in $\text{MLP}^{-/-}$ cells. Fig. 4C shows that neuraminidase also produced a negative shift in the voltage dependence of steady-state I_{Na} inactivation of WT but not $\text{MLP}^{-/-}$ cells. This change in the steady-state I_{Na} inactivation of neuraminidase-treated cells is similar to the one observed in $\text{MLP}^{-/-}$ myocytes. Finally, the rate of inactivation of I_{Na} in WT cells is slowed by more than 50% at negative potentials by the application of neuraminidase as shown in Fig. 4D. This slowing of

FIG. 3. Western blot analysis of the α -subunit of cardiac Na⁺ channels in WT and MLP^{-/-} hearts. A, Western blots show that the α -subunit of the cardiac Na⁺ channel has a lower apparent molecular weight in MLP^{-/-} than in WT heart. The image in this panel shows a representative Western blot of MLP^{-/-} (left lane) and WT (right lane) homogenates. Note that in addition to the Na⁺ channel smear above 203 kDa, the antibody produced a nonspecific band just above 110 kDa. This band was unchanging in WT and MLP^{-/-} samples and was used for normalizations (see "Materials and Methods"). B, densitometric scan of the region demarcated by the brace in A. The graph at the right shows a normalized densitometric scan of the specified region of the Western blot. The insets are bar plots of the mean \pm S.E. of the relative intensity (right) and relative width at 50% of the amplitude (left) of the Na⁺ channel band. The asterisk in these plots represents a statistically significant difference between the WT and MLP^{-/-}.



I_{Na} inactivation in WT cells is identical to the one observed in MLP^{-/-} cells. Neuraminidase did not affect the rate of inactivation of I_{Na} in MLP^{-/-} cells. These experiments show that, with respect to I_{Na} , neuraminidase treatment alone on WT cells produces results similar to those in HF. These data suggest that glycosylation of Na⁺ channels is altered in HF.

DISCUSSION

In this paper we have examined the electrical activity of hearts with contractile dysfunction. We found that in HF Na⁺ channel currents have shifted voltage dependences of activation and inactivation and slower rate of inactivation. Our results suggest that it is the reduction in Na⁺ channel glycosylation (α -subunit) that is responsible for the changes of I_{Na} properties. These provocative results raise a difficult question. Are the changes in I_{Na} consistent with the AP prolongation that is observed?

AP Prolongation—The data presented in this paper show that the acute reduction of Na⁺ channel glycosylation by neuraminidase can reproduce all of the changes in I_{Na} observed in heart failure except the following: the I_{Na} current density is not reduced. Our data suggest that this reduction in Na⁺ channel density in HF is produced by a reduction in the expression of functional Na⁺ channels. Most of the changes in I_{Na} that are observed in the MLP^{-/-} heart cell tend to reduce I_{Na} and thereby shorten AP duration. The one change that does tend to promote inward current (*i.e.* slowly inactivating I_{Na}) is over in less than about 10 ms and therefore has little direct effect on the APD. Thus, how can the AP prolongation observed in Fig. 1 be compatible with the characteristics of I_{Na} shown in Fig. 2? Wehrens *et al.* (16) addressed an identical question for a Na⁺ channel mutation that they were studying, the D1790G mutation.

In this case the D1790G mutation was found in patients who had a Na⁺ channel-dependent LQTS known as LQT-3. With the exception of this mutation, Wehrens *et al.* (16) noted that all other mutations of the cardiac Na⁺ channel that associated with LQTS resulted in an increase in the sustained component of I_{Na} . The D1790G mutation, however, produces a reduction in the sustained I_{Na} as was shown for the MLP^{-/-} heart cells. To examine this conundrum, Wehrens *et al.* (16) modified the

Luo/Rudy model (32, 33) of the cardiac AP to include changes in I_{Na} consistent with the D1790G mutation. They discovered that changes like those found in the D1790G mutation can lead to AP prolongation despite reduced AP "overshoot" and reduced maximum dV/dt of the AP upstroke. The model revealed that such alterations in I_{Na} can lead to increases in $[Ca^{2+}]_i$, and the prolongation of the AP was produced by the changes in Ca^{2+} . Thus, altered I_{Na} was paradoxically the cause of the AP prolongation in LQT-3. The changes in I_{Na} in HF are similar to those produced by the D1790G mutation in LQTS. Additionally, Fig. 5 shows that, in agreement with the model proposed by Wehrens *et al.* (16), the AP overshoot is less positive in MLP^{-/-} mouse ventricular myocytes (WT, 49.43 ± 2.36 mV, $n = 25$; MLP^{-/-}, 32.20 ± 4.15 mV, $n = 15$; $p < 0.05$), and the maximum rate of rise of the AP (dV/dt) is reduced in MLP^{-/-} myocytes. Ca^{2+} entry is increased when the APs have a slower rate of depolarization and a less positive peak because these changes increase the driving force for Ca^{2+} . A direct consequence of this increase in Ca^{2+} influx is that it will augment the inward Na⁺/Ca²⁺ exchanger current during the late stage of the AP and thereby prolong the AP (34). Taken together with the investigation of Wehrens *et al.* (16), these results suggest that the changes in I_{Na} seen in the MLP^{-/-} model of HF could significantly contribute to the AP prolongation observed and the associated EADs.

Post-translational Modification of the Cardiac Na⁺ Channels during Heart Failure—Data presented in this paper demonstrate that the deficient glycosylation of Na⁺ channels during heart failure produces an I_{Na} that has a slower rate of inactivation and shifted voltage dependencies of activation and inactivation. A mechanistic explanation of how negatively charged sialic acid particles on the external portion of Na⁺ channels contribute to the channel's voltage dependence is provided by the surface potential model (35, 36). According to this model, fixed, negatively charged particles (phospholipids and sugar residues) on the surface membrane of a cell produce a surface potential. The functional implication of this surface potential is that its magnitude determines the intra-membrane voltage, which is the voltage "sensed" by the voltage sensor of the Na⁺ channel; the smaller the surface potential, the smaller

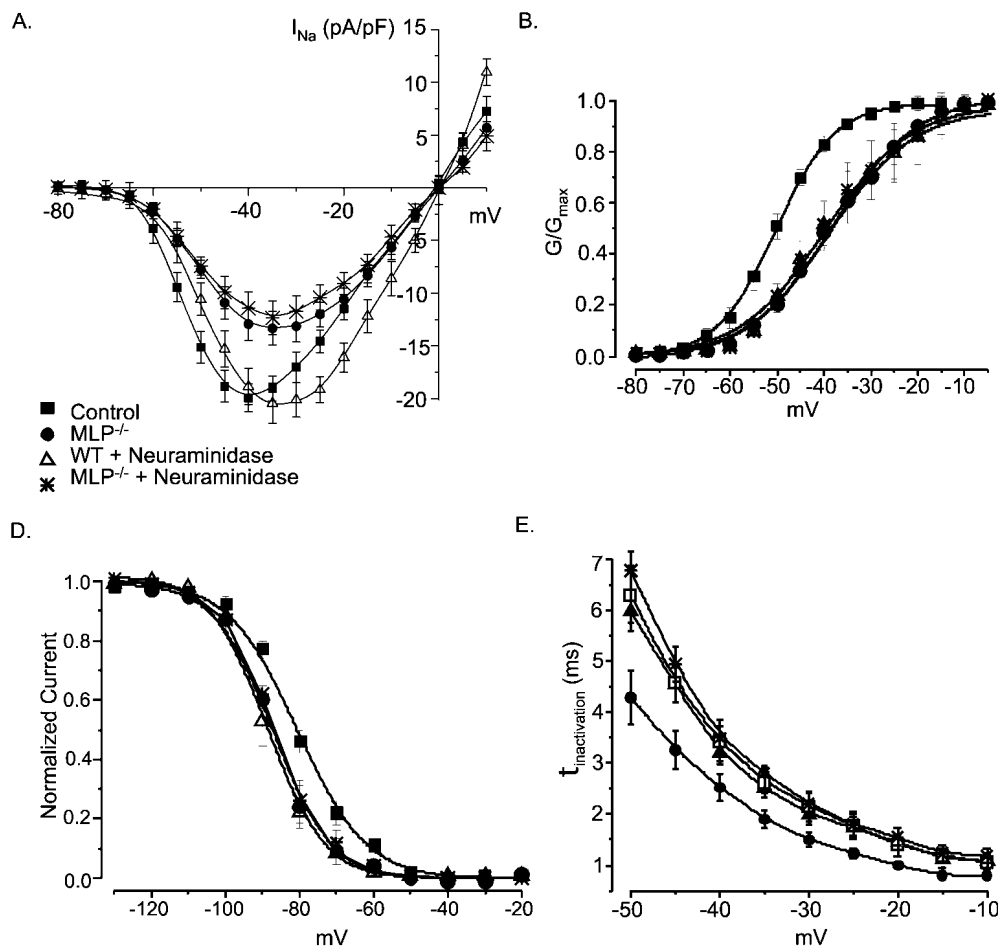


FIG. 4. **Enzymatic de-glycosylation of Na^{Na} channels in WT cells modifies I_{Na} and makes it similar to I_{Na} in $\text{MLP}^{-/-}$ cells.** *A*, IV relationship of I_{Na} in $\text{MLP}^{-/-}$ (●) and neuraminidase-treated WT (△) cells. *B*, voltage dependence of G/G_{max} of I_{Na} from WT and $\text{MLP}^{-/-}$ cells. The curves in this graph are the best-fit line determined by a least squares method using a Boltzmann equation equal to the one used in Fig. 2. The values of variables used in the Boltzmann equation to fit the $\text{MLP}^{-/-}$ data are provided in Fig. 2. For neuraminidase-treated WT myocytes, $A_1 = 1.01$, $A_2 = 0.02$, $V_{1/2} = -39.63$ mV, and $dV = 8.95$. *C*, voltage dependence of the steady-state inactivation of I_{Na} in $\text{MLP}^{-/-}$ (●) and neuraminidase-treated WT (△) cells. The voltage protocol used to generate these data is similar to the one used in Fig. 2. The curves in this graph are the best-fit line determined by a least squares method using a Boltzmann equation equal to the one used in Fig. 2. The values of the variables used in the Boltzmann equation used to fit the $\text{MLP}^{-/-}$ data are provided in Fig. 2. For neuraminidase-treated WT myocytes, $A_1 = 1.09$, $A_2 = 0.05$, $V_{1/2} = -88.75$ mV, and $dV = 6.75$. *D*, effects of neuraminidase on the rate of inactivation ($\tau_{\text{inactivation}}$) of I_{Na} in $\text{MLP}^{-/-}$ and NT WT cells. $\tau_{\text{inactivation}}$ was determined from the I_{Na} records used to generate *B* of this figure.

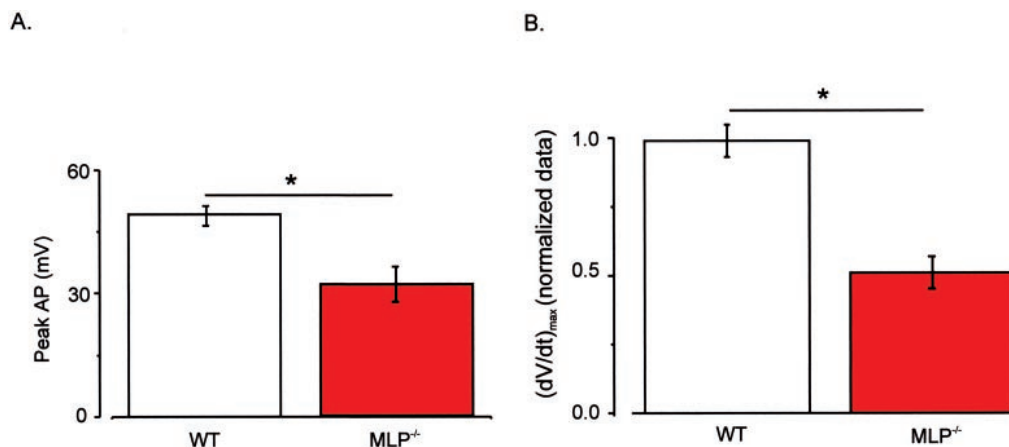


FIG. 5. **Arrhythmogenic changes in the AP of failing myocytes.** *A*, shown in this panel is a bar plot of the maximum amplitude of the AP peak in WT and $\text{MLP}^{-/-}$ myocytes. *B*, normalized maximum rate of depolarization of the AP in WT and $\text{MLP}^{-/-}$ myocytes. The * sign equals a $p < 0.05$.

the intra-membrane voltage and vice versa. Thus, reductions in the number of negative charges in the outer face of the plasma membrane, as would be produced by ion channel de-glycosylation or synthesis of sialic acid-deficient glycoproteins, have the effect of reducing the magnitude of the surface potential and

hence increase the intra-membrane potential. With a higher intra-membrane potential a greater membrane depolarization will have to occur for the channel to “sense” the same trans-bilayer field. The surface potential model thus predicts that a reduction in the number of negatively charged sialic acid resi-

dues linked to Na⁺ channels should produce a positive shift in the channel's threshold for activation.

It is intriguing to speculate on the possible mechanism by which Na⁺ channels are deficiently glycosylated during HF. One possibility is that the activity of sialyltransferase, the enzyme responsible for linking sialic acid to Na⁺ channel proteins in the Golgi apparatus, is reduced in MLP^{-/-} mice, which would lead to the production of sialic acid-deficient Na⁺ channels. Interestingly, the activity of sialyltransferase has been found to be reduced in a model of HF (21). Future experiments should examine if sialyltransferase activity is down-regulated in MLP^{-/-} myocytes and if this correlates with ion channel dysfunction. Our data suggest that the reduction in I_{Na} density observed in MLP^{-/-} cells results from a reduction in the number of functional Na⁺ channels expressed in these cells. Indeed, this conclusion is consistent with the observation that de-glycosylation of cardiac Na⁺ channels does not modify their unitary conductance (31). It would be interesting to examine whether this reduction in Na⁺ channel number results from a reduction in the abundance or translation of Na⁺ channel transcripts and/or a defect in the post-translational processing of these channels that promotes their rapid degradation.

We conclude that in the MLP^{-/-} model of HF, changes in the glycosylation of Na⁺ channel proteins during post-translational processing appear to be responsible for the changes in I_{Na} that lead to AP prolongation and the development of EPDs. Finally, it is intriguing to speculate that other ion channels and regulatory proteins in the heart may be subject to modification like the one observed for Na⁺ channels in HF.

Acknowledgments—We thank Dr. Walter Stuhmer for critically reading early versions of this paper and Dr. Jorge Miranda for preliminary experimental work.

REFERENCES

- Kannel, W. B., Plehn, J. F., and Cupples, L. A. (1988) *Am. Heart. J.* **115**, 869–875
- Esposito, G., Santana, L. F., Dilly, K., Cruz, J. D., Mao, L., Lederer, W. J., and Rockman, H. A. (2000) *Am. J. Physiol.* **279**, H3101–H3112
- Pak, P. H., Nuss, H. B., Tunin, R. S., Kaab, S., Tomaselli, G. F., Marban, E., and Kass, D. A. (1997) *J. Am. Coll. Cardiol.* **30**, 576–584
- Sanguinetti, M. C., Jiang, C., Curran, M. E., and Keating, M. T. (1995) *Cell* **81**, 299–307
- Kass, R. S., and Davies, M. P. (1996) *Cardiovasc. Res.* **32**, 443–454
- Satler, C. A., Walsh, E. P., Vesely, M. R., Plummer, M. H., Ginsburg, G. S., and Jacob, H. J. (1996) *Am. J. Med. Genet.* **65**, 27–35
- Russell, M. W., and Dick, M., II (1996) *Curr. Opin. Cardiol.* **11**, 45–51
- Sanguinetti, M. C., and Spector, P. S. (1997) *Neuropharmacology* **36**, 755–762
- Wilde, A. A., and Veldkamp, M. W. (1997) *Pacing Clin. Electrophysiol.* **20**, 2048–2051
- Wattanasirichaigoon, D., and Beggs, A. H. (1998) *Curr. Opin. Pediatr.* **10**, 628–634
- Kaab, S., Dixon, J., Duc, J., Ashen, D., Nabauer, M., Beuckelmann, D. J., Steinbeck, G., McKinnon, D., and Tomaselli, G. F. (1998) *Circulation* **98**, 1383–1393
- Kambouris, N. G., Nuss, H. B., Johns, D. C., Marban, E., Tomaselli, G. F., and Balsler, J. R. (2000) *J. Clin. Invest.* **105**, 1133–1140
- Bennett, P. B., Yazawa, K., Makita, N., and George, A. L., Jr. (1995) *Nature* **376**, 683–685
- George, A. L., Jr. (1996) *Nephrol. Dial. Transplant.* **11**, 1730–1737
- Wang, D. W., Yazawa, K., George, A. L., Jr., and Bennett, P. B. (1996) *Proc. Natl. Acad. Sci. U. S. A.* **93**, 13200–13205
- Wehrens, X. H., Abriel, H., Cabo, C., Benhorin, J., and Kass, R. S. (2000) *Circulation* **102**, 584–590
- Kass, R. S., Lederer, W. J., Tsien, R. W., and Weingart, R. (1978) *J. Physiol. (Lond.)* **281**, 187–208
- Pogwizd, S. M., Qi, M., Yuan, W., Samarel, A. M., and Bers, D. M. (1999) *Circ. Res.* **85**, 1009–1019
- Beuckelmann, D. J., Nabauer, M., and Erdmann, E. (1993) *Circ. Res.* **73**, 379–385
- O'Rourke, B., Kass, D. A., Tomaselli, G. F., Kaab, S., Tunin, R., and Marban, E. (1999) *Circ. Res.* **84**, 562–570
- Ma, T. S., Baker, J. C., and Bailey, L. E. (1979) *Cardiovasc. Res.* **13**, 568–577
- Arber, S., Hunter, J. J., Ross, J., Jr., Hongo, M., Sansig, G., Borg, J., Perriard, J. C., Chien, K. R., and Caroni, P. (1997) *Cell* **88**, 393–403
- Rockman, H. A., Chien, K. R., Choi, D. J., Iaccarino, G., Hunter, J. J., Ross, J., Jr., Lefkowitz, R. J., and Koch, W. J. (1998) *Proc. Natl. Acad. Sci. U. S. A.* **95**, 7000–7005
- Minamisawa, S., Hoshijima, M., Chu, G., Ward, C. A., Frank, K., Gu, Y., Martone, M. E., Wang, Y., Ross, J., Kranias, E. G., Giles, W. R., and Chien, K. R. (1999) *Cell* **99**, 313–322
- Zolk, O., Caroni, P., and Bohm, M. (2000) *Circulation* **101**, 2674–2677
- Santana, L. F., Kranias, E. G., and Lederer, W. J. (1997) *J. Physiol. (Lond.)* **503**, 21–29
- Knollmann, B. C., Knollmann-Ritschel, B. E., Weissman, N. J., Jones, L. R., and Morad, M. (2000) *J. Physiol. (Lond.)* **525**, 483–498
- London, B., Jeron, A., Zhou, J., Buckett, P., Han, X., Mitchell, G. F., and Koren, G. (1998) *Proc. Natl. Acad. Sci. U. S. A.* **95**, 2926–2931
- Baro, D. J., Ayali, A., French, L., Scholz, N. L., Labenia, J., Lanning, C. C., Graubard, K., and Harris-Warrick, R. M. (2000) *J. Neurosci.* **20**, 6619–6630
- Bennett, E., Urcan, M. S., Tinkle, S. S., Koszowski, A. G., and Levinson, S. R. (1997) *J. Gen. Physiol.* **109**, 327–343
- Zhang, Y., Hartmann, H. A., and Satin, J. (1999) *J. Membr. Biol.* **171**, 195–207
- Luo, C. H., and Rudy, Y. (1994) *Circ. Res.* **74**, 1097–1113
- Luo, C. H., and Rudy, Y. (1994) *Circ. Res.* **74**, 1071–1096
- Blaustein, M. P., and Lederer, W. J. (1999) *Physiol. Rev.* **79**, 763–854
- Frankenhaeuser, B., and Hodgkin, A. L. (1957) *J. Physiol. (Lond.)* **137**, 218–244
- Hille, B., Ritchie, J. M., and Strichartz, G. R. (1975) *J. Physiol. (Lond.)* **250**, 34–35

Role of Sodium Channel Deglycosylation in the Genesis of Cardiac Arrhythmias in Heart Failure

Carmen A. Ufret-Vincenty, Deborah J. Baro, W. Jonathan Lederer, Howard A. Rockman, Luis E. Quiñones and L. Fernando Santana

J. Biol. Chem. 2001, 276:28197-28203.

doi: 10.1074/jbc.M102548200 originally published online May 21, 2001

Access the most updated version of this article at doi: [10.1074/jbc.M102548200](https://doi.org/10.1074/jbc.M102548200)

Alerts:

- [When this article is cited](#)
- [When a correction for this article is posted](#)

[Click here](#) to choose from all of JBC's e-mail alerts

This article cites 0 references, 0 of which can be accessed free at <http://www.jbc.org/content/276/30/28197.full.html#ref-list-1>